CHROM. 12,798

CONTINUOUS FLOW ELECTROPHORESIS. THE CRESCENT PHENOMENA REVISITED

I. ISOTHERMAL EFFECTS

CORNELIUS F. IVORY

Separations Process Branch, Space Sciences Laboratory, MSFC, AL 35812 (U.S.A.)
(Received February 6th, 1980)

SUMMARY

Asymptotic solutions are derived for the partial differential equations (PDEs) governing solute behavior in the continuous flow electrophoresis device under isothermal operating conditions. In the limit, $D = 0$, analytical solutions are derived for the solute crescent shape and the concentration profile. In the limit, $((d/L)Pe_0)^{1/2} \gg 1$, an approximate solution to the PDE is found. These solutions are then used to predict the net dispersion of the concentration profile as a function of the fluid velocity in the chamber, the electrophoretic velocity of the solute and the electroosmotic flow at the chamber walls. The effects of diffusion on the net dispersion of the solute is also discussed for these limiting cases.

INTRODUCTION

In the current generation of continuous flow electrophoresis (CFE) devices a curtain of fluid is passed between two plates. An electric field is then established perpendicular to the direction of fluid motion and parallel to the plates. This allows a steady inlet stream of solute, introduced into the fluid curtain, to be fractionated according to its component electrophoretic mobilities. In this manner the inlet solute stream is continuously split into primary components and each component is collected separately at the outlet of the device.

Theoretical analysis of the concentration profiles in the CFE device has advanced in two main themes. The first of these, used by Strickler and Sachs[1], considers the non-diffusive limit of solute transport. The authors used their analysis to demonstrate the transport of solute in the electric field and, in particular, to elucidate the effects of electroosmotic flow at the chamber walls. Their work was qualitative in nature since it considered only the displacement of the solute stream and not the concentration profile of the exit stream. Their basic ideas have since been extended to predict solute concentration profiles using numerical procedures[2,3].

The second theme includes the effects of diffusion on the concentration profile[4]. This model is based on the usual equation of convection with diffusion and

includes electrophoretic migration orthogonal to the axis of convection. Although in principle this linear differential equation has an analytical solution, the fo m of the solution is very complicated. Reis *et al.*[4] propose an approximate solution based on the analysis of Gill and Sankarasubramanian[5] which considers the effects of diffusion along the three axes but ignores the effects of electroosmosis on the solute concentration profile.

While it is important to consider the effects of diffusion in the CFE analysis, the magnitude of the diffusive effect as compared with the electroosmotic effect is usually very small under normal operating conditions. In this paper two methods of calculating the concentration profiles in the CFE are described. The first is an analytical method for calculating the concentration profiles in the non-diffusive limit. The phenomenon of crescent formation is discussed in some detail along with general results from the analytical analysis. The second method is an approximate solution to the convection-diffusion equation which includes the effects of osmotic migration. This solution is compared with the solution of Reis *et al.*[4] in the limit as electro-osmosis becomes unimportant and to the analytical solution in the limit as diffusion becomes unimportant.

THEORETICAL

Convective dispersion in the CFE

In the absence of diffusion solute particles are assumed to follow the fluid and electrokinetic motions in their two respective axes. For the purposes of this study the left handed coordinate system of Saville and Ostrach[5] is used (see Fig. 1). The fluid
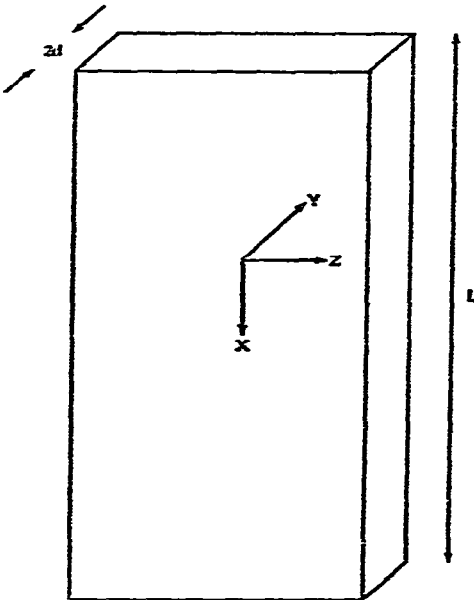

Fig. 1. Definitional sketch for the CFE device.

flow is in the positive x direction with maximum velocity V_M. The electrophoretic velocity is in the positive z direction as is the electroosmotic flow. Then the formulas for the velocities in the x and z directions are

$$V_x = i_x V_M (1 - y^2/d^2) \tag{1}$$

$$V_z = i_z \{ V_E - 3/2 V_E (1 - y^2/d^2) + U \} \tag{2}$$

where V_M is the maximum velocity in the x direction, V_E is the electroosmotic wall velocity and U is the solute electrophoretic velocity. Since the particles do not deviate from their characteristic fluid stream lines, the displacement of any particle along the z axis is determined by its net electrokinetic velocity multiplied by the solute holdup time,

$$\Delta = [U + V_E - \tfrac{3}{2} V_E (1 - y^2/d^2)] \cdot [L/V_M (1 - y^2/d^2)] \tag{3}$$

If a band of solute having thickness, 2δ, and width, γ, is continuously fed into the CFE at $x = 0$, then, as the solute is displaced along the z axis the forward and rearward points of the band itself deforms in the velocity field. The solute band may take on three distinct shapes depending on the conditions of operation of the CFE.
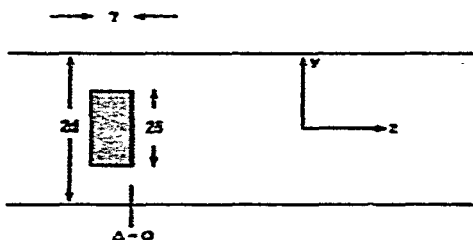

Fig. 2. Definitional sketch for the sample inlet of the CFE device.

(1) If $V_E = -U$ then the profile always appears as in Fig. 2 except that the band is displaced by $\Delta = 3/2\ UL/V_M$.

(2) If $V_E \neq -U$ and $\dfrac{V_M \gamma}{L} > \left| \dfrac{(U + V_E)\,(\delta/d)^2}{[1 - (\delta/d)^2]} \right|$ then

the cresent is "blunt" and the tail region has a constant concentration profile (see Fig. 3).

(3) If $V_E \neq -U$ and $\dfrac{V_M \gamma}{L} < \left| \dfrac{(U + V_E)\,(\delta/d)^2}{[(1 - (\delta/d)^2]} \right|$ then
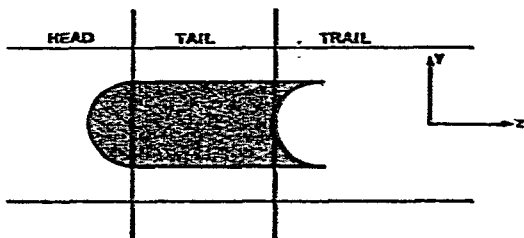

Fig. 3. Sketch of the "blunt" crescent showing the head, tail and trail regions.
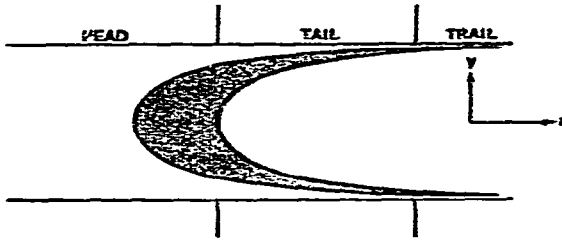
the crescent is "developed" (see Fig. 4).

Fig. 4. Sketch of the developed crescent showing the head, tail and trail regions.

The crescent formation is a natural artifact of band deformation due to the orthogonal flows in the CFE. If the solute has formed a crescent as viewed in the $y–z$ plane, then an analysis of the solute concentration (averaged over y) must be split into three parts. These parts are herein termed the crescent head, tail and trail. This is necessary because, when the solute input is rectangular in shape, integration across the y domain, $y\varepsilon(-1,1)$, is performed differently in each of the three regions. In the head, which occupies the region,

$$z\varepsilon\left(\frac{U+V_E}{V_M}L-\gamma,\ \frac{U+V_E}{V_M}L\right),$$

integration is performed from the centerline to the outer parabola. In the tail, which occupies the intermediate area between the head and the trail, integration is performed from the inner parabola to the outer parabola. And, in the trail, which occupies the region,

$$z\varepsilon\left(\left[\frac{U+V_E}{V_M(1-\delta^2/d^2)}-3/2V_E\right]L-\gamma,\ \left[\frac{U+V_E}{V_M(1-\delta^2/d^2)}-3/2V_E\right]L\right),$$

integration must be performed from the inner parabola to δ, the outer boundary of the solute inlet.

The boundaries of the inner and outer parabolas are determined from the formulas for the displacement, $\varDelta$. Solving eqn. 3 for y yields

$$y=\pm\left\{\frac{\frac{\varDelta}{L}+\frac{\frac{1}{2}V_E-U}{V_M}}{\frac{\varDelta}{L}+\frac{\frac{3}{2}V_E}{V_M}}\right\}^{1/2} \tag{4}$$

where the negative root is discarded. The parabola with its origin at $\varDelta-\gamma$ is given by the equation

$$y'=+\left\{\frac{\frac{\varDelta+\gamma}{L}+(\frac{1}{2}V_E-U)/V_M}{\frac{\varDelta+\gamma}{L}+\frac{3}{2}V_E/V_M}\right\}^{1/2} \tag{5}$$

Having determined the shape and the boundary of the solute profile, it is now possible to calculate the concentration of the solute in the fluid phase. There are two definitions of the concentration that have significance for the CFE. One is the concentration in the plane of viewing; that is, looking along the y axis into the x–z plane of the CFE as one might do with a photo-scanning device (see Krumrine[2]). The other is the solute flux through the plane of collection. This is the concentration which would be collected at each point along the z axis at the outlet of the CFE.

The concentration in the plane of viewing is defined as

$$\bar{C}(L, z) = {_0}\!\int^d C(L, y, z)\, dy \Big/ {_0}\!\int^d dy \tag{6}$$

The concentration in the plane of collection is defined as

$$\hat{C}(L, z) = {_0}\!\int^d N_x(L, y, z)\, dy \Big/ {_0}\!\int^d V_x\, dy \tag{7}$$

here

$$N_x(L, y, z) = V_x C(L, y, z) - D\, \frac{\delta C}{\delta x}\, (L, y, z) \tag{8}$$

The analytical solutions are useful in predicting solute behavior in the CFE without recourse to numerical methods. These solutions are limited because they only represent one geometry for the solute input, but they are still worth using as a first approach to column design and, as will be seen later in this paper, as an example of the limiting behavior in the CFE as diffusion becomes negligible.

For the case given above where the cresent is developed and the tail proceeds the head in the positive direction (*i.e.*, $V_E > -U$), these concentrations are

(1) In the head region,

$$z\varepsilon \left(\frac{U + V_E}{V_M} L - \gamma, \frac{U + V_E}{V_M} L \right)$$

$$\frac{\bar{C}}{C_0} = \left[\frac{(\Delta + \gamma) \cdot \frac{V_M}{L} + \frac{1}{2} V_E - U}{(\Delta + \gamma) \cdot \frac{V_M}{L} + \frac{3}{2} V_E} \right]^{1/2} \tag{9}$$

$$\frac{\hat{C}}{C_0} = \left[\frac{(\Delta + \gamma) \frac{V_M}{L} + \frac{1}{2} V_E - U}{(\Delta + \gamma) \cdot \frac{V_M}{L} + \frac{3}{2} V_E} \right]^{1/2} \left\{ \frac{(\Delta + \gamma) \frac{V_M}{L} + 2 V_E + \frac{U}{2}}{(\Delta + \gamma) \frac{V_M}{L} + \frac{3}{2} V_E} \right\} \tag{10}$$

(2) In the tail region

$$\frac{\bar{C}}{\bar{C}} = \left[\frac{(\Delta + \gamma) \frac{V_M}{L} + \frac{1}{2} V_E - U}{(\Delta + \gamma) \frac{V_M}{L} + \frac{3}{2} V_E} \right]^{1/2} - \left\{ \frac{\Delta \frac{V_M}{L} + \frac{1}{2} V_E - U}{\Delta \frac{V_M}{L} + \frac{3}{2} V_E} \right\}^{1/2} \tag{11}$$

$$\frac{\hat{C}}{C_0} = \left\{\frac{(\varDelta + \gamma)\frac{V_M}{L} + \frac{1}{2}V_E - U}{(\varDelta + \gamma)\frac{V_M}{L} + \frac{3}{2}V_E}\right\}^{1/2} \left\{\frac{(\varDelta + \gamma)\frac{V_M}{L} + \frac{1}{2}V_E + \frac{1}{2}U}{(\varDelta + \gamma)\frac{V_M}{L} + \frac{3}{2}V_E}\right\} -$$

$$-\left\{\frac{\frac{V_M}{L} + \frac{1}{2}V_E - U}{\varDelta\frac{V_M}{L} + \frac{3}{2}V_E}\right\}^{1/2} \left\{\frac{\varDelta\frac{V_M}{L} + 2V_E + \frac{1}{2}U}{\varDelta\frac{V_M}{L} + \frac{3}{2}V_E}\right\} \qquad (12)$$

(3) And in the trail region,

$$z\varepsilon\left(\left(\frac{U + V_E}{V_M\left(1 - \frac{\delta^2}{d^2}\right)} - \frac{3}{2}V_E\right)L - \gamma, \left(\frac{U + V_E}{V_M\left(1 - \frac{\delta^2}{d^2}\right)} - \frac{3}{2}V_E\right)L\right)$$

$$\frac{\bar{C}}{C_0} = \frac{\delta}{d} - \left\{\frac{\varDelta\frac{V_M}{L} + \frac{1}{2}V_E - U}{\varDelta\frac{V_M}{L} + \frac{3}{2}V_E}\right\}^{1/2} \qquad (13)$$

$$\frac{\hat{C}}{C_0} = \frac{1}{3}\frac{\delta}{d}\left(3 - \frac{\delta^2}{d^2}\right) - \left\{\frac{\varDelta\frac{V_M}{L} + \frac{1}{2}V_E - U}{\varDelta\frac{V_M}{L} + \frac{3}{2}V_E}\right\}^{1/2} \left\{\frac{\varDelta\frac{V_M}{L} + 2V_E = \frac{1}{2}U}{\varDelta\frac{V_M}{L} + \frac{3}{2}V_E}\right\} \qquad (14)$$

The effects of diffusion in the CFE

When diffusion of solute is included in the analysis of the concentration profiles in the CFE, the system is then described by the usual equation of diffusion with convection and electrophoretic migration. The general form of this differential equation is

$$V_x(y)\frac{\delta C}{\delta x} + (U + V_E(y))\frac{\delta C}{\delta z} = D\left(\frac{\delta^2 C}{\delta x^2} + \frac{\delta^2 C}{\delta y^2} + \frac{\delta^2 C}{\delta z^2}\right) \qquad (15)$$

with the boundary conditions that

$$
\begin{array}{ll}
y = \pm d & \delta C/\delta y = 0 \\
z = \pm\infty & C = 0 \\
x = 0 & C = C_0\delta(z) \\
x = \infty & C \text{ is finite}
\end{array}
\qquad (16)
$$

Using the dimensionless parameters

$$
\begin{array}{ll}
x^* = x/d & \text{Pe}(y^*) = V_x(y^*)d/D \\
y^* = y/d & \text{El}(y^*) = [U + V_z(y^*)]\,d/D \\
z^* = z/d & C^* = C/C_0
\end{array}
$$

which then gives the dimensionless form of the equation

$$\text{Pe}(y^*)\frac{\delta C^*}{\delta x^*} + \text{El}(y^*)\frac{\delta C^*}{\delta z^*} = \frac{\delta^2 C^*}{\delta x^{*2}} + \frac{\delta^2 C^*}{\delta y^{*2}} + \frac{\delta^2 C^*}{\delta z^{*2}} \tag{17}$$

with boundary conditions that

$$
\begin{array}{ll}
y^* = \pm 1.0 & \delta C^*/\delta y^* = 0 \\
z^* = \pm \infty & C^* = 0 \\
x^* = 0 & C^* = \delta(y^*) \\
x^* = +\infty & C^* \text{ is finite}
\end{array}
\tag{18}
$$

In order to simplify the mathematics of this problem it is desired to eliminate the term describing diffusion along the y axis. The explanation for doing this is intuitive in nature and is given immediately below where λy is the mean diffusional displacement along the y axis.

$$\frac{\lambda_y}{d} = \frac{(2Dt)^{1/2}}{d} = \left(\frac{(L/d)}{\text{Pe}(y^*)}\right)^{1/2} \ll 1.0 \tag{19}$$

When this criterion is met, diffusional spreading along the y axis of the chamber is very small compared to the thickness, d, of the chamber. Dispersional spreading along the z^* axis due to the movement of solute from the center of the chamber becomes small compared to the dispersion due to convective influences, although it probably remains slightly more important than diffusion along the other two axes. The net result of this assumption is that the concentration in the vicinity of the peak is slightly overestimated with the leading edge of the curve somewhat overextended, the tail behind the peak is underestimated and the farthest edge of the tail is overestimated since the solute would diffuse toward the center of the chamber as well as along the x and z axes and, sampling the higher velocities, it would leave the chamber sooner. Thus, concentration profiles generated from this approximate solution give a conservative overestimate of the diffusive effect on dispersion in the CFE.

It is instructive to point out that in the limit of no diffusion we have already seen that the solute concentration profile peak exits the CFE chamber at $z = (\text{Pe}_0/\text{El}_0)x$. In the limit as diffusion dominates convective transport the solute is able to frequently sample all positions on the y axis and so the peak will exit the column at $z \cong \frac{1}{2}(\text{Pe}_0/\text{El}_0)x$ since each particle travels through the chamber at the average fluid velocity. This means that as operating conditions go from low diffusion to high diffusion effects there is a shift of 50% in the displacement of the peak from the origin. This will be important later in discussing the results of Reis.

The equation to be solved then is

$$\frac{\delta^2 C^*}{\delta x^{*2}} + \frac{\delta^2 C^*}{\delta z^{*2}} = \text{Pe}(y^*)\frac{\delta C^*}{\delta x^*} + \text{El}(y^*)\frac{\delta C^*}{\delta z^*}. \tag{20}$$

Using the transform

$$C^*(x^*,y^*,z^*) = f(x^*,y^*,z^*) \exp(\text{Pe}(y^*)x^* + \text{El}(y^*)z^*)/2 \tag{21}$$

reduces the differential equation to

$$\frac{\delta^2 f}{\delta z^{*2}} + \frac{\delta^2 f}{\delta x^{*2}} = \left[\frac{\text{Pe}^2(y^*) + \text{El}^2(y^*)}{4}\right] f \tag{22}$$

This equation automatically satisfies the boundary conditions on y^*. The conditions on x^* and z^* are

$$
\begin{aligned}
x^* &= \pm \infty & f &= 0 \\
z^* &= 0 & f &= \delta(y^*) \\
z^* &= \infty & f &= 0
\end{aligned}
\tag{23}
$$

Because the domain of x is semi-infinite the fourier sine transform may be used where

$$
F_x(f) = \left(\frac{2}{\pi}\right)^{1/2} \int_0^\infty f(x) \sin(sx)\, dx
\tag{24}
$$

$$
f(x) = \left(\frac{2}{\pi}\right)^{1/2} \int_0^\infty F_x(f) \sin(sx)\, ds
\tag{25}
$$

and the fourier exponential transform is used in z.

$$
F_e(f) = {}_{-\infty}\!\int^{+\infty} f(y) \exp + (i\alpha y)\, dy
\tag{26}
$$

$$
f(y) = \frac{1}{2\pi} {}_{-\infty}\!\int^{+\infty} F_e(f) \exp - (i\alpha y)\, d\alpha
\tag{27}
$$

which yields the double transform

$$
F_s(Fe(f)) = s/(\alpha^2 + s^2 + \gamma^2)
\tag{28}
$$

where $\gamma^2 = (Pe^2(y^*) + El^2(y^*))/4$ and $K_1(z)$ is a modified Bessel function of the second kind of order one.

The solution for the concentration profile in the CFE is then

$$
C^*(x^*, y^*, z^*) = \frac{(2\pi)^{-1/2}\, \gamma x^*}{(x^{*2} + z^{*2})^{1/2}} K_1(\gamma(x^{*2} + z^{*2})^{1/2}) \exp\left(\frac{(Pe\, x^* + El\, z^*)}{2}\right)
\tag{29}
$$

Calculations of the concentration in the plane of viewing and concentration through the plane of collection are generated from formulas 6 and 7, respectively. The integrations are done numerically and the results are presented in the next section.

RESULTS

The solution generated in this manner is approximate and so it is helpful to compare it with other extant solutions. For this purpose the functions generated by Reis et al.[4] are shown here as well as the analytic solutions generated earlier in this paper. The results of Reis et al. are for the special case when the CFE chamber walls do not generate an osmotic flow. The form of that solution gives the concentration in the plane of collection. Because both of these approximate solutions use a Dirac function for the solute input they cannot be directly compared to the analytical solution in the non-diffusive limit. For this reason the input width, and concentration of the analytical solution are modified so that the height and width of the output correspond roughly to the diffusive spreading if there were no electric field.

In Fig. 5 a comparison is made of the solution of Reis *et al.*[4] and the solution given in this paper at Peclet numbers of 20 and 100 when there is no imposed electric field. Agreement between these results is good although the Reis solution is consistently higher over the z axis. This may be due to the fact that Reis' solution, as is
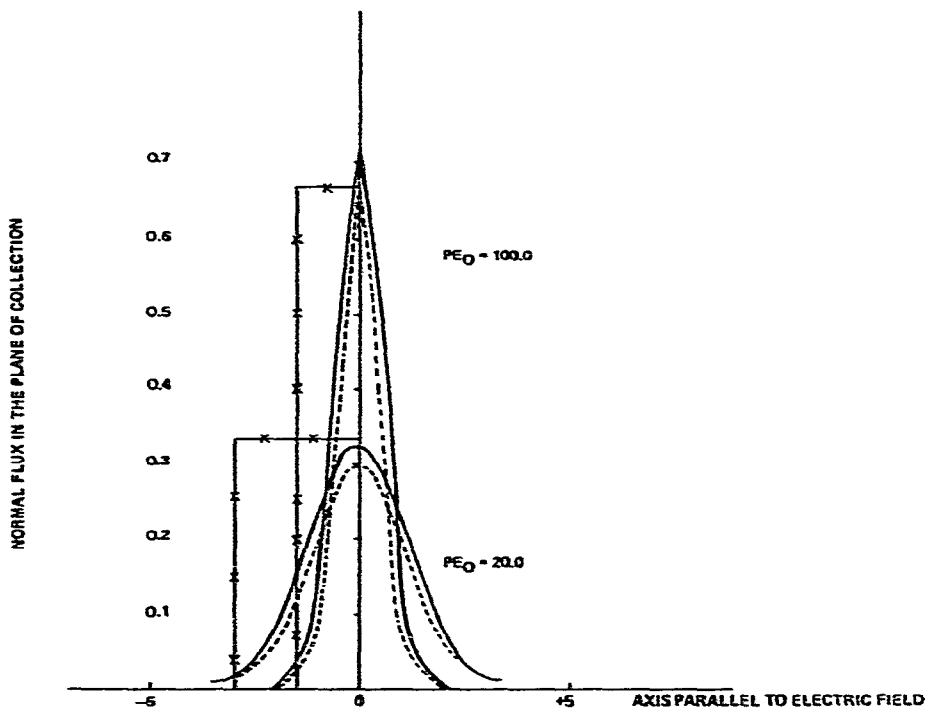

Fig. 5. A comparison of Reis' solution to the solutions derived in this paper when there is no applied electric field. —•—, Analytical solution ($D = 0$); ——, Reis' solution; - - -, this work. $L/d = 10.0$; $U/V_M = 0.0$; $V_E/V_M = 0.0$.

stated in his paper, is not normalized whereas the solution generated in this paper is normalized. Figs. 6 and 7 are a comparison, at Peclet numbers of 20 and 100, of the two solutions when an electrophoretic velocity is included in the solution. In Fig. 6 it is immediately apparent that the peak locations differ between the two solutions. Fig. 7 demonstrates that an increase in the Peclet number has opposite effects on these two solutions. Reis' solution predicts that increasing the Peclet number leads to increased dispersion while this work shows a decrease in dispersion.

This peculiar behavior of Reis' solution was predicted in his paper[4] and, in fact, further calculations show that his solution actually goes through a minimum in dispersion for $0 < Pe_0 < 100$ when $L = 10$. No explanation for this behavior is offered in his paper and none is given here (Fig. 8).

Figs. 9 and 10 are a comparison of Reis' solution, the solution from this paper and the analytical solution in the limit of zero diffusion for $Pe = 20, 100$ and $L = 100$. The last two solutions show very good agreement in the position of their peaks and
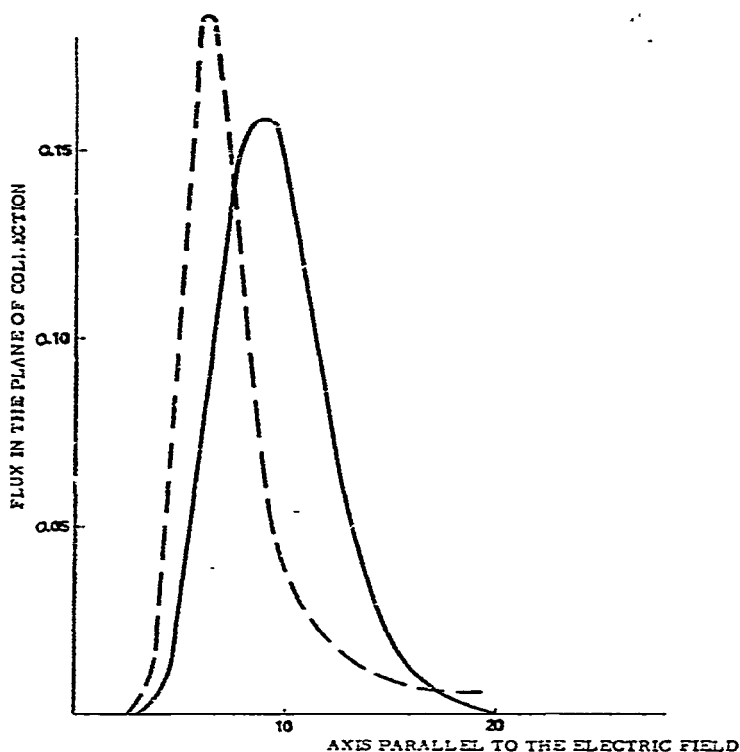
Fig. 6. A comparison of Reis' solution with the solution derived in this paper at a Peclet number of 20 with no electroosmotic flow. ——, Reis' solution; – – –, this work. $U/V_M = 0.6$; $L/d = 10.0$; $Pe_0 = 20.0$; $V_E/V_M = 0.0$.

in their respective trailing dispersions. The third solution is displaced from the first two by nearly 50% and otherwise has no resemblance to the analytical result.

It is apparent from the graphical work presented here that Reis' solution differs substantially from the solutions presented in this paper. Reis' solution does not reduce to the analytic solution in the limit as $(Pe_0 d/L)^{\frac{1}{2}} \rightarrow \infty$ as do the other solutions. There are two important points which suggest a reason why this happens.

In the first place, the elution peak arrives at a position on the z axis associated with the average fluid velocity rather than the maximum fluid velocity. In the limit as $(Pe_0 d/L)^{\frac{1}{2}}$ is large the latter would be true while for small $(Pe_0 d/L)^{\frac{1}{2}}$ the former would be expected.

Secondly, Reis et al. assert that the parameter

$$\alpha = \langle CV \rangle / \langle C \rangle \langle V \rangle = \hat{C}/\bar{C} \tag{30}$$

has a value that is never very different from 1.0. This would be expected at low values of $(Pe_0 d/L)^{\frac{1}{2}}$ since the solute would manage to frequently sample all positions on the y axis, but as may be seen from the zero diffusion results
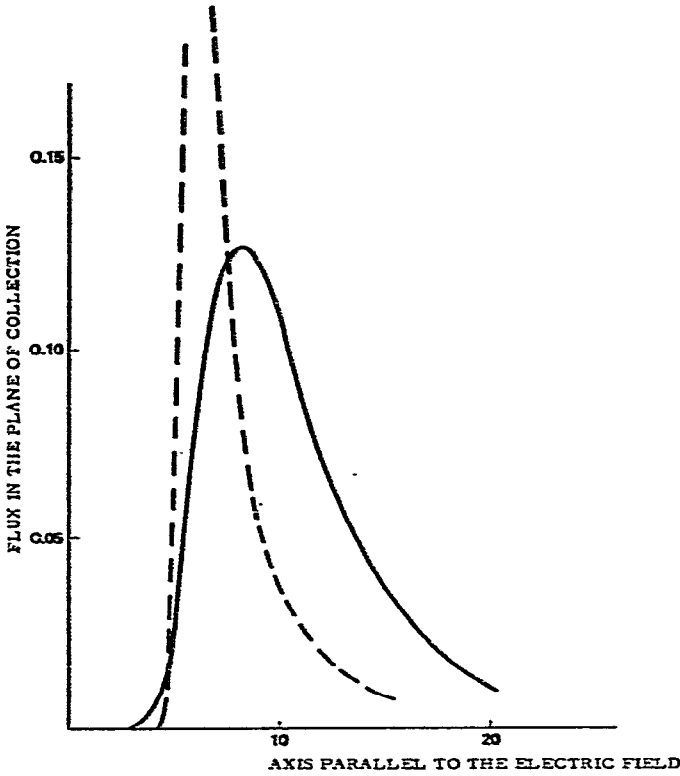
Fig. 7. A comparison of Reis' solution with the solution derived in this paper when the Peclet number is 100 and there is no electroosmotic flow. ——, Reis' solution; – – –, this work. $U/V_M = 0.6$; $L/d = 10.0$; $Pe_0 = 100.0$; $V_E/V_M = 0.0$.
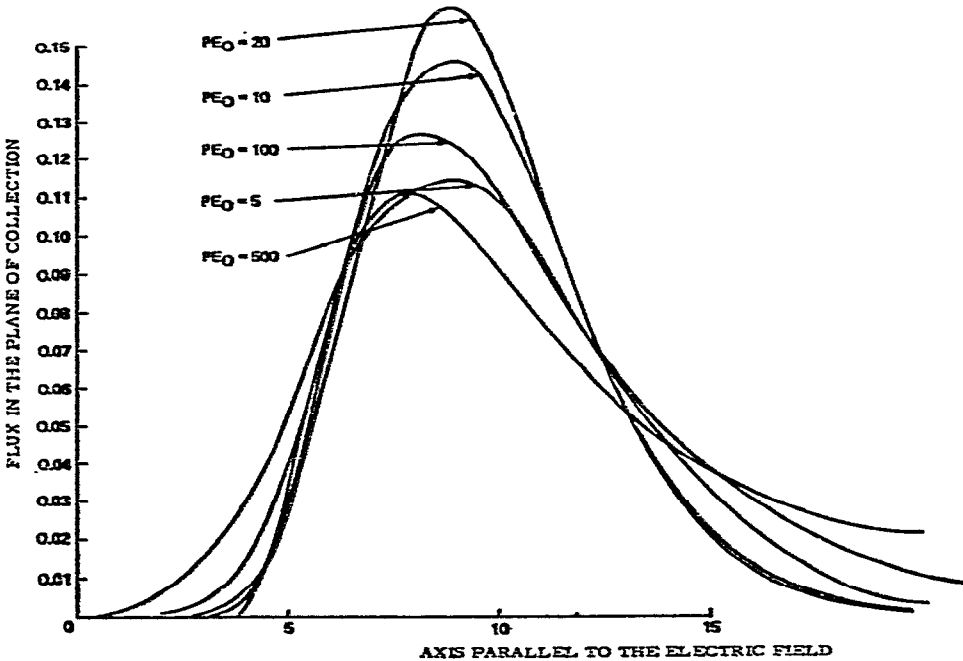

Fig. 8. The effect of the Peclet number on the dispersion of the solute using Reis' solution. $U/V_M = 0.6$; $L/d = 10.0$; $V_E/V_M = 0.0$.
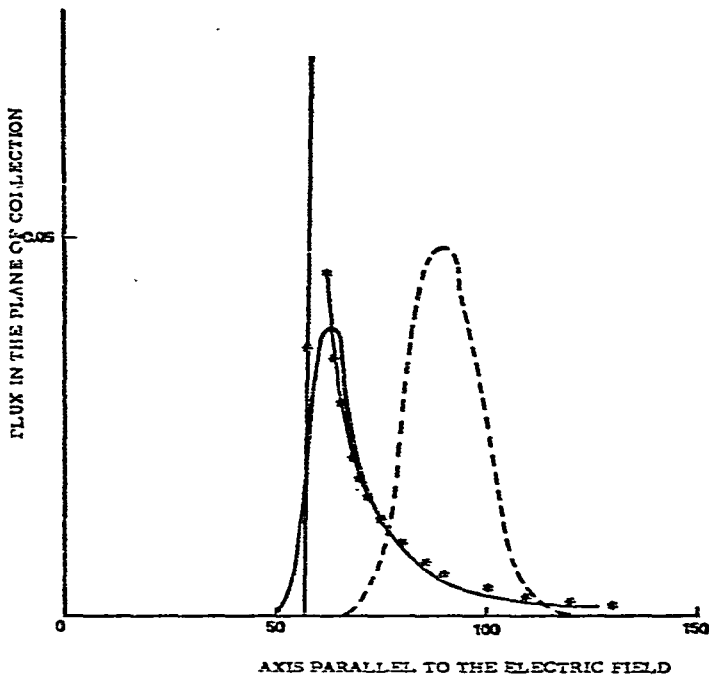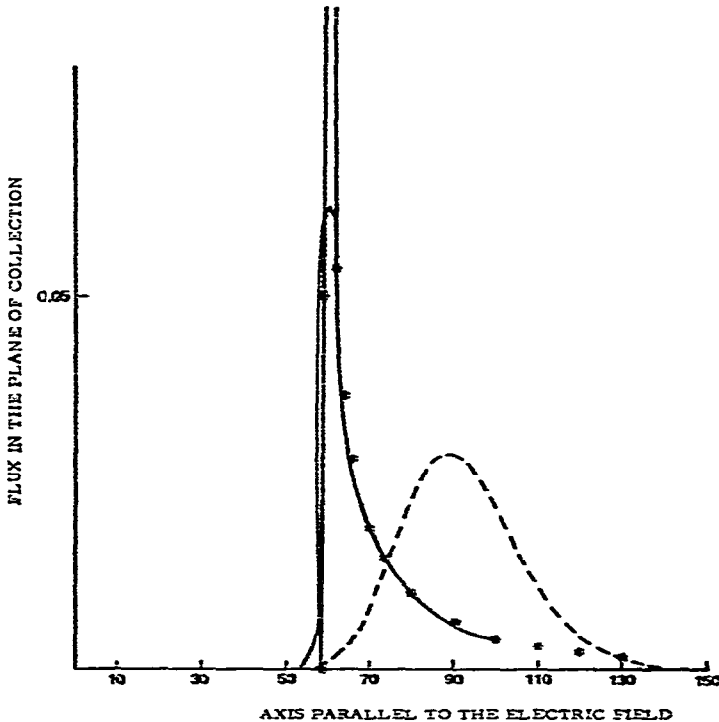
Fig. 9. A comparison of Reis' solution with the solutions derived in this paper when the non-dimensional column length is 100 and the Peclet number is 20. —*—, Analytical solution; – – –, Reis' solution; ——, this work. $U/V_M = 0.6$; $L/d = 100.0$; $Pe_0 = 20.0$; $V_E/V_M = 0.0$.

Fig. 10. A comparison of Reis' solution with the solutions derived in this paper when the non-dimensional column length is 100 and the Peclet number is 100. —*—, Analytical solution; – – –, Reis' solution; ——, this work. $U/V_M = 0.6$; $L/d = 100$; $Pe_0 = 100.0$; $V_E/V_M = 0.0$.

$$\frac{\hat{C}}{\bar{C}} = \frac{\frac{3}{2}U + \gamma \frac{V_M}{L}}{U + \gamma \frac{V_M}{L}}$$
(31)

at the peak of the elution curve. The maximum value of α is 1.5 when γ is small. These two points together suggest that the solution of Reis *et al.* is only valid at low values of $(Pe_0 d/L)^{\ddagger}$.

Fig. 11 shows the effect of increasing the Peclet number on the dispersion of the concentration profile. From this figure it is apparent that there is no minimum in the dispersion of the solute with increasing Peclet number. Also, a very slight shift is noticeable in the position of concentration peak.
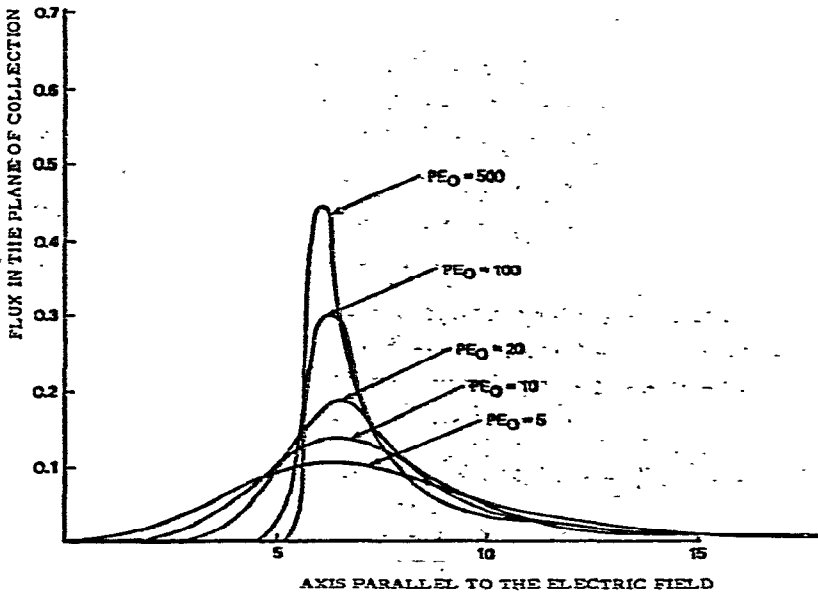

Fig. 11. The effect of the Peclet number on dispersion in the approximate solution derived in this paper. $U/V_M = 0.6$; $L/d = 10.0$; $V_E/V_M = 0.0$.

The profiles shown in Fig. 12 include the effect of an osmotic wall velocity. They clearly show the beneficial effects of operating the CFE such that $U = -V_E$. Finally, Fig. 9 is a graph of the crescents formed by the profiles in Fig. 13. It is the crescent formation phenomena which contribute the majority of the dispersion to the solute concentration profile. Notice that when $U = -V_E$ the crescent shape is not formed but diffusive influences cause the solute to assume an hourglass configuration.

CONCLUSIONS

The results of the latter part of this paper must be interpreted carefully and only in the light of the assumptions used in the solution of the problem. The heuristic
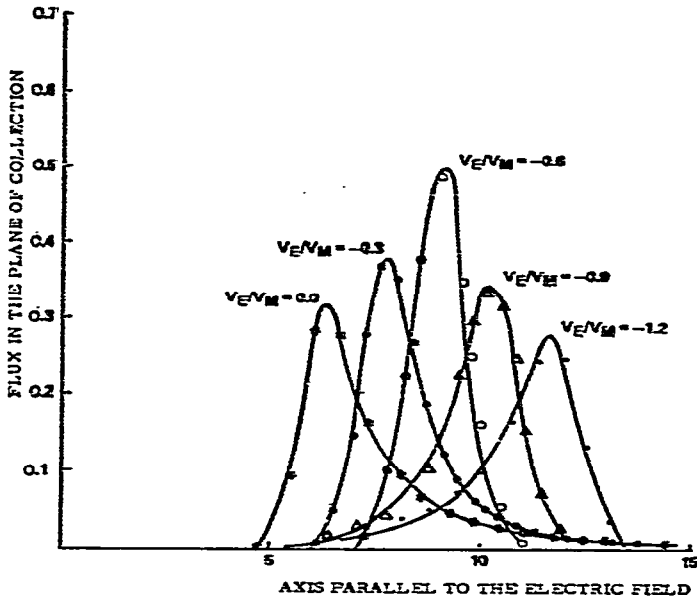
Fig. 12. The effect of electroosmotic velocity on dispersion using the approximate solution derived in this paper. $L/d = 10.0$; $Pe_0 = 100.0$; $U/V_M = 0.6$.
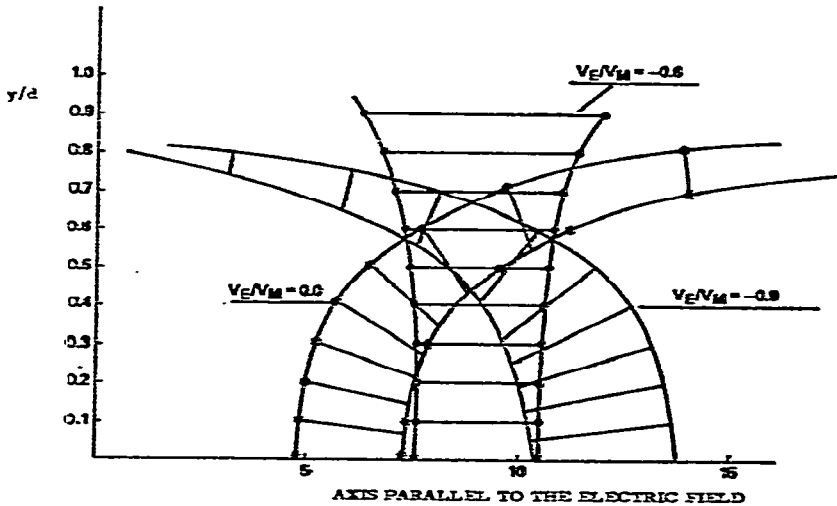

Fig. 13. The effect of the electroosmotic velocity on the formation of crescent when the effect of diffusion is included. Notice that the crescent in the center, $V_E/V_M = -U/V_M$, has an hourglass shape rather than a typical crescent shape. $U/V_M = 0.6$; $Pe_0 = 100.0$; $L/d = 10.0$.

application of mathematic approximations for simplification's sake can only be justified, in this case, by the accuracy of these results when they are studied in their asymptotic limit, $(Pe_0 d/L)^{\pm} \to \infty$. From these results we are able then to extract some useful information.

In the first place these equations predict a phenomenon as yet undetected in operating devices. This is the formation of an hourglass configuration of solute in the chamber slit. Again it is important that the results here only slightly overestimate the diffusive effect and so this phenomenon is not just an artifact of the calculation.

Secondly, the results point out the shortcomings of the earlier work done by Reis *et al*. While it may be that the error in their analysis is due simply to truncation of their analysis, the solution presented in their paper is clearly inapplicable to CFE operation at high values of $(Pe_0d/L)^{\ddagger}$. In this limit the approximate solution presented here agrees very well with the analytical solutions presented in the first part of the paper. These solutions adequately describe the synergetic effects of the parabolic fluid and osmotic velocities on the dispersion of solute in the CFE chamber.

ACKNOWLEDGEMENT

REFERENCES

1 A. Strickler and T. Sacks, *Prep. Biochem.*, 3 (1973) 269.
2 P. H. Krumrine, *Ph.D. Thesis*, Lehigh University, Bethlehem, PA, 1978.
3 J. A. Gionnovario, R. N. Griffin and E. L. Gray, *J. Chromatogr.*, 153 (1978) 329.
4 J. F. Reis, E. N. Lightfoot and H. Lee, *AIChE J.*, 20 (1974) 363.
5 D. Saville and S. Ostrach, *The Fluid Mechanics of Continuous Flow Electrophoresis*, Final Report, Contract NAS8-31349, Code 361, MSFC, AL, 1978.